**Manuscript**
**Click here to view linked References**

# High temperature reactions of water with heavy oil and bitumen: insights into aquathermolysis chemistry during steam-assisted recovery.

**Wren Montgomery[1]*, Richard W. Court[1], Andrew C. Rees[2] and Mark A. Sephton[1]**

1) *Department of Earth Science and Engineering, South Kensington Campus, Imperial College London, London SW7 2AZ.*

2) *BP America Production Company, 501 Westlake Park Boulevard, Houston, Texas, 77079. USA.*

*Corresponding author; w.montgomery@imperial.ac.uk, Tel.: +44(0)2075945185, Fax: +44(0)2075947444

Prepared for *Fuel*

## Abstract

To better understand the hot water-mediated organic transformation process (aquathermolysis) that occurs during the steam-assisted recovery of heavy oils and bitumen we have performed a series of experiments that subject a heavy oil to progressively higher temperatures and pressures in the presence of liquid water. As temperature and pressure increases, from ambient conditions to 300 °C and 1250 psig (8.6 MPa), a floating oil (flotate) is generated and is composed of mostly aliphatic hydrocarbons that appear to be generated at the expense of polars and asphaltenes. Analyses of hopane maturity parameters for the flotate indicate lower temperatures than the starting material suggesting the liberation of hopanes and, therefore, other hydrocarbons, from asphaltenes. Infrared spectra confirm changes in overall organic constitution as the relative abundance of hydrocarbons to oxygen-containing functional groups increases in the flotate. At the highest temperatures and pressures (325 °C, 1750 psig (13.8 MPa)) the flotate is at a maximum relative amount, the untransformed heavy oil is at a minimum and significant amounts of methane are generated indicating the onset of cracking. Steam-assisted recovery of heavy oil, therefore, leads to changes in the chemical constitution of a number of chemical fractions generating a lighter oil and gases that must be taken into account when planning field operations for production.



**Keywords:** aquathermolysis, SAGD, high pressure

## 1. Introduction

Heat and water are known modifiers of organic matter but the particular type of organic transformation observed can be dependent on the conditions under which modification has taken place. When heat, with or without water, leads to the decomposition of organic matter it is termed pyrolysis [1]. Anhydrous pyrolysis is the thermal decomposition of organic matter in a water-free environment while hydrous pyrolysis has been defined as those conditions in which the heated samples are in contact with liquid water for the duration of the experiment. Supercritical water pyrolysis denotes experiments in which a sample is pyrolyzed in contact with a supercritical fluid containing more than 50 mole % water [2] while steam pyrolysis indicates experiments in which a sample is pyrolyzed in contact with water vapour at partial pressures in excess of 20 % of its saturated vapour pressure [2]. Hydrous, supercritical, and steam pyrolysis are all covered by the umbrella terms hydrothermal pyrolysis or aquathermolysis, e.g. [3].

The influence of water is perhaps most profound when considered in relation to processes for the generation and exploitation of fossil fuels. When compared to anhydrous conditions, pyrolysis of organic-rich shales in the presence of water produces organic products that are physically, chemically and isotopically more similar to natural crude oils suggesting a closer replication of natural subsurface maturation conditions [4]. Moreover, hydrous pyrolysis experiments display product yields that are greater, by up to 100%, than in comparable anhydrous experiments [5] [6]. When water is present, its state represents an important control on pyrolysis product yields [7]; historical data reveal that steam reduced yields of oil from oil shale during retorting [8] whereas liquid water increased the yield of soluble materials from heated coals by an order of magnitude [9]. Experimental data also reveal that ratios of water to organic compounds can exert an influence on product yields; for example ratios between 2.5:1 and 5:1 are optimal for hydrolysis reactions [10].

Hydrous pyrolysis studies have been widely applied to simulating the production of crude oil in the subsurface [4]. Crude oil is a staple energy resource and accounts for over 35% of the world's energy consumption but the demand for refined products is outstripping the supply of conventional oil and so focus is turning to unconventional hydrocarbon deposits. One such unconventional hydrocarbon deposit is represented by heavy oil and bitumen where "technical reserves," those which are technically viable although not necessarily commercially viable today, total > 1 trillion bbl where a large proportion will likely require (*in situ*) steam stimulation for production [11]. A good example of this is the province of Alberta in Canada which has 169 billion bbl of crude bitumen reserves (technically and commercially viable today using steam-assisted *in situ* recovery methods) which is just 9% of the initial volume in place; in 2011 Alberta produced on average 630,000 bbl/day of bitumen through steam stimulation methods and this rate is expected to triple by 2021 [12].

The role of water in organic transformation has been studied in relation to heavy oil and bitumen primarily because of the use of steam and water in recovery [13] [14]. Steam injection into the sub-surface has been used for decades to assist the recovery of heavy oil primarily through three methods: steam-flooding, Cyclic Steam Stimulation (CSS), and more recently Steam-Assisted Gravity Drainage (SAGD). Operating temperatures and pressures used in these methods differ widely, but SAGD temperatures are typically 180 – 240 $^{o}$C and CSS can operate at temperatures in excess of 300 $^{o}$C. These processes all offer intimate contact between the oil, condensed water and mineral matter for residence times of multiple days permitting even slow chemical processes to produce quantifiable changes to the oil and the generation of significant quantities of gas. Even using the simplest model, these processes can be seen to involve a number of variables that will change over distance and time, including: i) temperature ii) phase, iii) water/oil ratio and iv) opportunity for static vs. dynamic reaction conditions. More complex

85 variables involve the chemistry of the starting materials, e.g. [15], and mineralogy of the
86 reservoir rocks, e.g. [16].

87 Owing to its ability to produce high yields of lower molecular weight products from higher
88 molecular weight starting materials, the area of the steam chamber which is experiencing
89 hydrous pyrolysis is perhaps most interesting. A key consideration is that, with respect to both
90 economics and engineering, maintaining hydrous pyrolysis conditions over large areas of the
91 steam chamber is more plausible compared to other higher temperature pyrolysis conditions
92 involving water. Hydrous pyrolysis studies that aim to provide insights into steam-assisted
93 recovery processes should ideally be comprehensive in that all of the solid, liquid and gaseous
94 material is monitored during the experiments. For instance, untransformed residues are related
95 to the recovery efficiency while gas contents could reflect diagnostic products of aqueous or
96 thermal chemical reactions. Gas contents also reveal whether these processes will generate any
97 production engineering issues owing to acid gas generation (hydrogen sulphide and carbon
98 dioxide). Inevitably this approach involves multiple analytical instruments. Previous hydrous
99 pyrolysis experiments on source rocks have demonstrated the utility of studies that are
100 comprehensive and partially [17] or fully [7] quantitative.

101 In this paper we report on a series of hydrous pyrolysis experiments. A sample of well-
102 characterised biodegraded heavy oil was subjected to various temperatures and pressures.
103 Although the experiment durations are relatively short, it is expected that the reactions that
104 take place will reflect those occurring in the presence of liquid water across the temperature
105 and pressure gradients experienced in steam-assisted recovery. These data indicate the
106 progressive transformation of organic matter with temperature through different bond breaking
107 events to produce an increasingly less viscous oil. Higher temperatures also lead to greater

quantities of gas. The gas becomes progressively more hydrocarbon-rich at higher temperatures. Organic transformations are relatively concentrated into specific chemical fractions. The data provide insights into how management of steam-assisted processes can lead to in situ changes in heavy oil.

## 2. Experimental

### *2.1. Samples*

For the oil sand extraction experiments, degraded oil in a sand matrix was obtained from Osmington Mills, Dorset, United Kingdom. Although by no means an economic prospect, the oil sand provides a well-characterized analogue for study. Examination of the cliff face at Osmington Mills (Grid Reference: 50.63391°N, 2.37571°W) reveals clays, limestones and sandstones of Upper Jurassic age. At sea level, the six metre thick Bencliff Grits are found and comprise fine grained sands with occasional mudstone layers. Large scale cross bedding, dewatering structures and the presence of land plant material suggest rapid sedimentation in a near shore setting [18]. The sands exhibit porosities of 15-20% and permeabilities of 10-1000 mDa [19]. The Bencliff Grits display a notable and widespread oil stain the most likely source of which is the Lower Jurassic Blue Lias shales which contain marine type II kerogen. Tertiary inversion in the Wessex Basin resulted in the breach of the Bencliff Grit oil accumulation to produce a sulfur-poor heavy oil with densities in the 18.4-18.9° API range [20] and a viscosity of 1538 Pa·s at 25°C.

### *2.2. Hydrous pyrolysis*

Approximately 50 g of Osmington Mills sample were added to a high pressure and temperature reactor (Model 4740, Parr Instruments). Using the measured reactor volume, 75 ml, and calculated sample density, and the pressure required, the mass of water needed was determined and added. The remaining headspace within the reactor was purged with nitrogen

and the reactor was sealed and placed in an oven for 24 hours. Pressure was monitored throughout the experiment using a dedicated pressure gauge attached to the reactor. Subcritical water experiments were performed on samples of oil sands at a range of temperatures and pressures as follows: 30 °C, 0 psig; 250 °C, 600 psig; 275 °C, 800 psig; 300 °C, 1250 psig; 325 °C, 1750 psig.

### *2.3. Post experiment sampling*

Once the experiment was complete and the reactor cooled, gases were extracted from the reactor headspace by releasing a needle gauge and allowing the gas to flow into a chamber with a septum. Gas was collected from this chamber using a gas-tight syringe. The gas quantities in the syringe were scaled to reveal the total quantities in the reactor headspace. Following gas sampling, the reactor was opened and any oil floating on the surface of the water (the flotate) was transferred to a test tube using a polytetrafluoroethylene (PTFE)-coated spatula. To isolate any water-soluble organic matter, the reactor contents were drained into test tubes, aided by rinsing with deionised water. The test tubes were centrifuged at 500 rpm for 20 minutes to settle any suspended material, then the supernatant was pipetted off. Two cycles of further addition of deionised water, centrifugation and pipetting followed. The separated water, containing the water-soluble fraction of the subcritical water treatment products, was subjected to liquid-liquid extraction with dichloromethane (DCM). This consisted of the addition of DCM and sonication for 15 minutes at 40% amplitude, using a Sonics & Materials, Inc. VCX-130 Vibra-Cell sonicator, followed by centrifugation and pipetting off the supernatant. Two further cycles of addition of DCM, centrifugation and pipetting followed, then the DCM was allowed to evaporate to produce a water-soluble oil fraction (the liquid-liquid extract). The residual oil still coating the sand residues was extracted with 93:7 (vol:vol) DCM:methanol(MeOH) for 15 minutes, followed by centrifugation and collection of the supernatant as described above.

### *2.4. Total organic carbon contents*

To measure the total organic carbon (TOC) content, 100 mg of sample was weighed and introduced to 0.5 M HCl solution in order to remove any carbonate present (x2) before washing with high purity water. The sample was dried and inserted into a LECO Corporation carbon analyzer where it was heated in a furnace to 1000 °C in the presence of oxygen. The organic carbon was oxidised to carbon dioxide, the quantity of which was measured by an InfraRed cell already calibrated on samples of known carbon content. TOC measurements were made for the oil sands before and after the subcritical water experiment. An additional measurement was made after the further DCM/MeOH extraction step. All experimental residues were allowed to dry in an oven at 50 °C prior to analysis.

### *2.5. FTIR spectroscopy*

Gas in the gas-tight syringe was inserted into a Chemical Data Systems (CDS) Analytical Brill Cell™ attached to a Thermo-Nicolet 5700 FTIR spectrometer. The cell was purged with helium (BOC Grade A, 99.996% purity) at a flow rate of 20 ml $s^{-1}$ for several seconds prior to gas insertion. FTIR spectra were collected at a resolution of 4 $cm^{-1}$ using a mercury cadmium telluride (MCT-A) detector, cooled by liquid nitrogen. Liquid residues and extracts were measured using a Smart Orbit™ attenuated total reflectance (ATR) accessory attached to the same Thermo-Nicolet 5700 FTIR spectrometer. Samples were dissolved in the appropriate solvent and a drop was placed on the diamond analysis crystal, with the solvent then left to evaporate. Spectra were produced by the accumulation of 32 spectra, both for the background and the sample using a deuterated triglycine sulphate detector at a resolution of 4 $cm^{-1}$.

### *2.6. Fractionation*

Samples of the flotates and DCM/MeOH-soluble fractions were further separated into saturate (aliphatic), aromatic, resin (polar) and asphaltene (collectively termed SARA) fractions.

Asphaltenes were precipitated from the sample using a 30-fold excess of heptane with a 12 hour settling time; further separation was achieved by centrifugation. The precipitation process was repeated three times in total. The maltene fraction was further separated into aliphatic, aromatic and polar fractions using alumina micro-column chromatography. The aliphatic fraction was eluted with hexane, the aromatic fraction with DCM, and the polar fraction with MeOH. Fractions were allowed to dry at room temperature and pressure before being weighed.

### *2.7. Gas chromatography-mass spectrometry*

Aliphatic and aromatic fractions were re-dissolved in DCM at a concentration of 1 g $l^{-1}$ and analysed using an Agilent 6890N gas chromatograph (GC) and a 5973 Mass Selective Detector. One µl of solvent was injected in to the DB-5MS column, with helium carrier gas flowing at 1.1 ml $min^{-1}$. The GC oven was initially held at 50 °C for 1 minute, then the temperature raised at 4 °C $min^{-1}$ to 310 °C, where it was held for 20 minutes, for a total run length of 86 minutes. The standards were identified by reference to the NIST 05 mass spectral database, and the retention times for this instrumental configuration established by previous runs of the individual standards.

## 3. Results and Discussion

Results from the hydrous pyrolysis experiments are presented as a series of tables (Tables 1 to 6) and Figures (Figures 1 to 7) that display the amounts and organic chemical nature of various fractions before and after hot water treatment including the total organic carbon contents of the oil sand, the gas contained in the headspace of the high temperature reactor, the flotate, the liquid-liquid extracts of experiment water and the DCM/MeOH extracts of the experimental residue. The relatively abundant flotates and DCM/MeOH extracts of the experimental residue were also chromatographically subdivided and analysed as their aliphatic, aromatic, polar and

asphaltene fractions. Many of the various fractions display concordant trends and the data are best discussed by reference to distinct sets of experimental temperatures and pressures.

### *3.1. Room temperature and pressure*

At room temperature and pressure the Osmington Mills oil sand contains 8.79% TOC and 11.13% of extractable organic matter (EOM%). When immersed in water some of the oil dissolves in the water and is recoverable by liquid-liquid extraction but most remains associated with the mineral matrix and is recovered by extraction with DCM/MeOH (Figure 1). No flotate (or gas) forms at room temperature and pressure. The relative abundances of the various fractions in the Osmington Mills starting material reveal that aliphatic material is the most dominant fraction with aromatic, polar and asphaltene materials making up roughly equal parts of the remainder (Figure 2). FTIR spectra of the Osmington Mills starting material added to water at room temperature and pressure is displayed in Figure 3. In both the liquid-liquid extract of the water and solvent extract of the residual sand strong absorption bands are present at 2900 $cm^{-1}$, 1375 $cm^{-1}$ and 1455 $cm^{-1}$ and represent methyl and methylene C-H bonds. Absorption by carbonyl C=O bonds is apparent around 1710 $cm^{-1}$, while aromatic C-C bonds are assigned to the band around 1600 $cm^{-1}$. The band around 1100 $cm^{-1}$ is attributed to C-O bonds in alcohols.

GCMS data of the aliphatic fraction (Figure 4) reveal that substantial degradation has taken place in the natural environment with the loss of all straight chain hydrocarbons. A large unresolved complex mixture provides a response from m/z 55 indicating the presence of cyclic alkanes. Hopanes and steranes are still visible in the total ion current chromatogram suggesting that biodegradation was arrested before all source signals were destroyed. Mass chromatograms for *m*/*z* 191 (Figure 5) reveal further details on the hopane content of the oil. As noted by previous authors, the Osmingon Mills oil also contains no 25-norphopane produced by microbial demethylation of hopanes that would have indicated biodegradation at depth so the

current state of the oil is most likely dependent on surface alteration [21]. The hopane composition of Osmington Mills starting material has been studied previously [18]; our measurement of the $C_{31}$ 22S/22S+22R maturity parameter at 0.684 is slightly above their report of 0.556-0.596 for directly sampled oil seeps.

### *3.2. 250 °C and 600 psig to 300 °C and 1250 psig*

Progressively higher temperatures and pressures leads to a general decrease in TOC% in the experimental residue before solvent extraction (Table 2). The post solvent extraction TOC% is greater than seen in the starting material at room temperature and pressure and steadily increases with temperature and pressure. The appearance and progressive increase in solvent insoluble material may reflect coke formation [[22]. Within the temperature/pressure range studied in this report, the 250 °C and 600 psig step marks the onset of flotate production. As temperature and pressure increases the flotate displays a steady growth in the relative abundance of aliphatic and to some extent aromatic material and a corresponding decrease in the relative abundance of polar material.

The SARA data from this study is in harmony with previously published data from solvent extracted natural bitumens and those generated by hydrous pyrolysis experiments. In all circumstances the major variation in SARA data occurs because of changes in the relative abundance of aliphatic and polar/asphaltene fractions[7]. It is possible that a major control on the relative abundance of aliphatic and polar fractions is the maturity-driven loss of heteroatomic functional groups to leave behind the aliphatic skeletons.

Interpretations that involve defunctionalization of polars to produce aliphatic materials are supported by the FTIR data (Figure 3) Comparison of the ratios of band intensities in a sample can provide information regarding the changes in the relative abundance of functional groups as

251 temperatures and pressures increase. Variations indicate a series of changes as responses from
252 aliphatic material increases relative to the responses from oxygen-containing functional groups
253 and, therefore, polar material (Figure 3).

254 FTIR spectra of the gas extracts from the samples following hydrous pyrolysis are shown in
255 Figure 3. The spectra contain strong absorptions from carbon dioxide (a doublet at 2350 $cm^{-1}$)
256 and weaker absorption from methane around 3015 $cm^{-1}$. Defunctionalization of polar material
257 would lead to the production of carbon dioxide and that this reaction product is seen to increase
258 in relative abundance in the collected headspace gases (Figure 3) further supports the concept
259 of progressive transformation of polar materials with increasing temperature and pressure.
260 Methane becomes progressively more important as temperature and pressure increases (Figure
261 7). At 275 °C and 800 psig the production of methane increases by an order of magnitude
262 compared to the lower temperature and pressure step. The Osmington Mills sample is known to
263 contain little sulfur so hydrogen sulfide was not observed; for samples with high sulfur contents,
264 sulfur-bearing gases would be observed with this technique.

265 GC-MS data for the flotates generated display a noticeable relative increase in unresolved
266 complex mixture (UCM) components that elute at lower retention times compared to the
267 starting material and the DCM/MeOH extract of the experiment residue (Figure 5). The lack of
268 discrete peaks in the total ion currents imply that the flotate components are branched and
269 cyclic aliphatic compounds. The few discrete peaks above the UCM at higher retention times are
270 hopanes and steranes allowing an examination of changes in maturity parameters with
271 increasing pressure and temperature. Figure 6 reveals that the maturity of the flotate, as
272 reflected by the $C_{32}$ hopane S/S+R maturity parameter, falls rapidly away from that of the initial
273 sample. The minimum apparent maturity occurs at 275 °C, 800 psig, suggesting the recharge of

free hopanes from the asphaltene fraction and the possibility that the "natural" maturity parameter ratio has been enhanced by biodegradation. The DCM:MeOH extracts of the experimental residue exhibit less systematic changes in maturity parameters.

### *3.3. 325 °C and 1750 psig*

The 325 °C and 1750 psig step reflects a dramatic increase in flotate production and a minimum in solvent soluble material. It is most likely that these high temperatures and pressures have induced cracking, removing most solvent-soluble organic matter from the oil sand. Solvent insoluble material is at a maximum and may reflect coke formation. At this relatively high temperature and pressure the flotate displays a maximum relative abundance of aliphatic material and a minimum relative abundance of polar material and reflects a continuation of the defunctionalization process observed in the lower temperature and pressure steps.

Carbon dioxide is present after all heating experiments but is most pronounced in the 325 °C and 1750 psig experiment. High temperatures and pressures are associated with carbon-carbon bond breaking [23]. Repeated carbon-carbon bond breaking will produce progressively smaller hydrocarbons and ultimately methane. Figure 5 shows the evolution of methane with temperature. The 325 °C and 1750 psig FTIR data reveal that high temperatures and pressures generate significant amounts of methane. Under these conditions, the $C_{32}$ hopane S/S+R maturity parameter of the flotate approaches the initial value (Figure 6), indicating that biomarkers released from asphaltenes during hydrous pyrolysis are equilibrating to similar levels of thermal stress experienced by the original oil.

### *3.4. Implications for steam-assisted recovery*

Manipulation of temperature and pressure of water in the steam chamber can lead to the in situ transformation of heavy oil. At 250 °C and 600 psig to 300 °C and 1250 psig the oil becomes increasingly dominated by the economically preferred aliphatic material at the expense of polar

material and asphaltenes. During this process a small amount of intractable material is generated alongside the gaseous by-products of molecular transformation, carbon dioxide, water and methane (and hydrogen sulfide for oils which contain sulfur). At 325 °C and 1750 psig there is a step change in the yield of aliphatic material which is an order of magnitude greater than previous steps and the production of methane continues. The data in this paper allow predictions to be made for the chemical transformations that occurs during steam assisted recovery and the types of gases that accompany these processes allowing an assessment of the engineering difficulties brought about by specific thermal and aqueous conditions.

## 4. Conclusions

Data from the hydrous pyrolysis experiments on Osmington Mills oil sands reveal that treatment at relatively low temperatures and low pressures (250 °C and 600 psig) has a dramatic effect on the chemistry of heavy oil, defunctionalizing the polar organic compounds present to produce a lighter oil richer in aliphatic hydrocarbons and a gas phase containing carbon dioxide. With sufficient agitation, the lighter oil floats on top of the extracting water. The maturity parameters of the flotate indicate lower temperatures than the starting material suggesting the recharge of hopanes from asphaltenes. Experimental data also indicate that higher temperatures and pressures progressively increase the relative abundance of hydrocarbons over functionalized organic matter up to 325 °C and 1750 psig. At this relatively high temperature and pressure cracking occurs, removing most solvent-soluble organic matter from the oil sand, generating a maximum amount of floating light oil. Significant quantities of methane are generated during all experiments at and above 275 °C and 800 psig. The data provide insights into how management of steam-assisted processes can lead to in situ changes in heavy oil and the generation of associated gases that add complexity to field operations during production.

## 5. References


[1] W.J. Irwin, Analytical Pyrolysis - An overview, Journal of Analytical and Applied Pyrolysis, 1 (1979) 3-25.

[2] M.D. Lewan, Nomenclature for pyrolysisexperimentsinvolving $H_2O$, American Chemical Society Division of Fuel Chemistry Preprints, 37 (1992) 1545–47.

[3] A.R. Katritzky, S.M. Allin, M. Siskin, Aquathermolysis: Reactions of organic compounds with superheated water, Accounts of Chemical Research, 29 (1996) 399-406.

[4] M.D. Lewan, J.C. Winters, J.H. McDonald, Generation of oil-like pyrolyzates from organic-rich shales, Science, 203 (1979) 897-899.

[5] P.A. Comet, J. McEvoy, W. Giger, A.G. Douglas, Hydrous and anhydrous pyrolysis of DSDP Leg 75 kerogens—A comparative study using a biological marker approach, Organic Geochemistry, 9 (1986) 171-82.

[6] M.D. Lewan, Laboratory simulation of petroleum formation – hydrous pyrolysis, in: M. Engel, S. Macko (Eds.) Organic Geochemistry Principles and Applications, Plenum Press, New York, 1993, pp. 419–42.

[7] M.D. Lewan, Experiments on the role of water in petroleum formation, Geochimica et Cosmochimica Acta, 61 (1997) 3691-723.

[8] M.J. Gavin, Oil-shale--an historical, technical, and economic study, U.S. Bureau of Mines Bulletin, 210 (1922) 179-89

[9] F. Fischer, The conversion of coal into oil, Ernest Berm Ltd., 1925.

[10] J.W. King, R.L. Holliday, G.R. List, Hydrolysis of soybean oil in a subcritical water flow reactor, Green Chemistry, 1 (1999) 261-4.

[11] Hart-Energy-Research-Group, Heavy Crude Oil: A Global Analysis and Outlook to 2035, 2011.

[12] Energy-Resources-Conservation-Board, Alberta's Energy Reserves 2011 and Supply/Demand Outlook 2012-2021, 2012.

[13] P.D. Clark, J.B. Hyne, J.D. Tyrer, Chemistry of organosulphur compound types occurring in heavy oil sands: 1. High temperature hydrolysis and thermolysis of tetrahydrothiophene in relation to steam stimulation processes, Fuel, 62 (1983) 959-62.

[14] P.D. Clark, J.B. Hyne, J. D. Tyrer, Some chemistry of organosulphur compound types occurring in heavy oil sands: 2. Influence of pH on the high temperature hydrolysis of tetrahydrothiophene and thiophene, Fuel, 63 (1984) 125-8.

[15] T. Barth, Similarities and differences in hydrous pyrolysis of biomass and source rocks, Organic Geochemistry, 30 (1999) 1495-507.

[16] H. Fan, Y. Zhang, Y. Lin, The catalytic effects of minerals on aquathermolysis of heavy oils, Fuel, 83 (2004) 2035-9.

[17] T.I. Eglinton, A.G. Douglas, S.J. Rowland, Release of aliphatic, aromatic and sulphur compounds from Kimmeridge kerogen by hydrous pyrolysis: A quantitative study, Organic Geochemistry, 13 (1988) 655-63.

[18] D.F. Watson, A.D. Hindle, P. Farrimond, Organic geochemistry of petroleum seepages within the Jurassic Bencliff Grit, Osmington Mills, Dorset, UK, Petroleum Geoscience, 6 (2000) 289-97.

[19] G. Watts, R. Belford, T. Melling, Record breaking wells in the land of the great crested newt, Petroleum Exploration Society of Great Britain field trip., 1998.

[20] G.M. Lees, P.T. Cox, The geological basis of the present search for oil in Great Britain by the D'Arcy Exploration Company Limited, Journal of the Geological Society, 93 (1937) 156-94.

[21] C. Cornford, O. Christie, U. Endresen, P. Jensen, M.-B. Myhr, Source rock and seep oil maturity in Dorset, Southern England, Organic Geochemistry, 13 (1988) 399-409.

[22] J. Towfighi, M. Sadrameli, A. Niaei, Coke formation mechanisms and coke inhibiting methods in pyrolysis furnaces, J. Chem. Eng. Jpn., 35 (2002) 923–47.

[23] M.D. Lewan, Laboratory simulation of petroleum formation by hydrous pyrolysis, in: M.H. Engel, S.A. Macko (Eds.) Organic Geochemistry, Plenum Press, New York, 1993, pp. 419-422.

## Figure Captions

**Figure 1.** Histograms displaying the relative abundance (%) of flotate, water soluble organic matter and solvent-recoverable organic matter at the various temperatures and pressures.

**Figure 2.** Histograms displaying the relative abundance (%) of saturate (aliphatic), aromatic, resin (polar) and asphaltene (collectively termed SARA) fractions.

**Figure 3.** FTIR spectra showing responses from starting materials and products from hydrous pyrolysis experiments. In the gas products, carbon dioxide is most prominent with a doublet at 2350 $cm^{-1}$, along with a weak signal from methane at 3000 $cm^{-1}$. In the liquid products, the group of bands around 3000 $cm^{-1}$ are produced by absorption from methyl and methylene C-H bonds: 2950 $cm^{-1}$ methyl C-H, 2920 $cm^{-1}$ methylene C-H, 2870 $cm^{-1}$ methyl C-H and 2850 $cm^{-1}$ methylene C-H. Methyl C-H also produces the weaker band at 1375 $cm^{-1}$; methylene C-H is the source of the 1455 $cm^{-1}$ band. The band around 1710 $cm^{-1}$ is attributed to carbonyl C=O bonds, and the band around 1600 $cm^{-1}$ is attributed to aromatic C-C bonds.

385 Bands around 1100 $cm^{-1}$ result from absorption by C-O bonds in alcohols. The relative abundance of
386 aliphatic and oxygen-containing functional groups vary between fractions and with increasing
387 temperature and pressure.

388 **Figure 4.** GC-MS Total ion current chromatograms for the aliphatic fractions of the Osmington Mills
389 starting material and its hydrously pyrolyzed products.

390 **Figure 5.** GC-MS m/z 191 mass chromatograms for the aliphatic fractions of the Osmington Mills starting
391 material and its hydrously pyrolyzed products.

392 **Figure 6.** a) $C_{32}$ hopane S/S+R maturity parameters of the aliphatic fractions of the Osmington Mills
393 starting material and its hydrously pyrolyzed products. b) Averaged $C_{32}$ hopane S/S+R maturity
394 parameters over $C_{30}$-$C_{35}$ hopanes. Error bars from the standard deviation of these values.

395 **Figure 7.** FTIR spectra showing the progressive increase in methane with temperature and pressure.

396

## Tables

Table 1. Oil sand total organic carbon (TOC%) and extractable organic matter (EOM%). Note that the EOM can display larger values than TOC because the former contains elements other than carbon.

| Sample | TOC (%) | n | EOM% | δ | n |
|---|---|---|---|---|---|
| OM 2009 | 8.79 | 1 | 11.13 | ± 0.44 | 3 |

Table 2. Total organic carbon (%) of experimental residues

| Temperature | Pressure | Starting | | Post expt | | Post solvent | |
|---|---|---|---|---|---|---|---|
| (ºC) | (psig) | TOC% | (%) | TOC% | (%) | TOC% | (%) |
| 30 | 0 | 8.79 | 100 | --- | --- | 0.21 | 0.02 |
| 250 | 600 | 8.79 | 100 | 8.82 | 100 | 1.31 | 0.15 |
| 275 | 800 | 8.79 | 100 | 8.12 | 92 | 1.51 | 0.17 |
| 300 | 1250 | 8.79 | 100 | 7.06 | 80 | 1.12 | 0.17 |
| 325 | 1750 | 8.79 | 100 | 9.65 | 100 | 0.96 | 0.2 |

Table 3. Sample details, and masses and yields of the extractable phases. Note that the yields are expressed as percentages of the whole rock starting material.

| Conditions | | Start material | | Flotate | | Liquid-liquid extract | | Solvent extract | | Total liquid extract | |
|---|---|---|---|---|---|---|---|---|---|---|---|
| Temp (ºC) | Press (psig) | Mass (g) | TOC (%) | Mass (g) | Yield (%) | Mass (g) | Yield (%) | Mass (g) | Yield (%) | Mass (g) | Yield (%) |
| 30 | 0 | 50.24 | 8.79 | 0 | 0 | 0.25 | 0.5 | 5.38 | 10.72 | 5.63 | 11.21 |
| 250 | 600 | 50.10 | 8.79 | 0.23 | 0.46 | 0.02 | 0.04 | 3.36 | 6.71 | 3.62 | 7.22 |
| 275 | 800 | 50.10 | 8.79 | 0.22 | 0.43 | 0.08 | 0.16 | 3.73 | 7.45 | 4.02 | 8.03 |
| 300 | 1250 | 50.30 | 8.79 | 0.05 | 0.11 | 0.01 | 0.02 | 4.08 | 8.10 | 4.14 | 8.22 |
| 325 | 1750 | 50.33 | 8.79 | 1.05 | 2.08 | 0.02 | 0.04 | 3.1 | 6.16 | 4.15 | 8.25 |

Table 4. Aliphatic, polar, aromatic and asphaltene fractions of flotates and DCM:MeOH extracts.

| | 30 C, 0psig | 250 C, 600 psig | | 275 C, 800 psig | | 300 C, 1250 psig | | 325, 1750 psig | |
|---|---|---|---|---|---|---|---|---|---|
| | DCM:MeOH | Flotate | DCM:MeOH | Flotate | DCM:MeOH | Flotate | DCM:MeOH | Flotate | DCM:MeOH |
| Aliphatics | 41 | 29 | 10 | 28 | 11 | 33 | 18 | 43 | 16 |
| Polars | 15 | 22 | 19 | 25 | 18 | 23 | 16 | 15 | 13 |
| Aromatics | 14 | 10 | 19 | 13 | 11 | 19 | 16 | 22 | 18 |
| Asphaltenes | 30 | 39 | 52 | 34 | 60 | 25 | 50 | 20 | 53 |

Table 5. $C_{32}$ S/S+R hopane maturity parameters.

| 30 C, 0 psig | 250 C, 600 psig | | 275 C, 800 psig | | 300 C, 1250 psig | | 325, 1750 psig | |
|---|---|---|---|---|---|---|---|---|
| DCM:Me | Flotate | DCM:MeOH | Flotate | DCM:MeOH | Flotate | DCM:MeOH | Flotate | DCM:MeOH |
| 0.627 | 0.617 | 0.599 | 0.570 | 0.592 | 0.584 | 0.590 | 0.606 | 0.580 |

Table 6. $C_{30}$-$C_{35}$ S/S+R hopane maturity parameters.

| 30 C, 0 psig | 250 C, 600 psig | | 275 C, 800 psig | | 300 C, 1250 psig | | 325, 1750 psig | |
|---|---|---|---|---|---|---|---|---|
| DCM:MeOH | Flotate | DCM:MeOH | Flotate | DCM:MeOH | Flotate | DCM:MeOH | Flotate | DCM:MeOH |
| 0.635±.009 | 0.603±.011 | 0.608±.02 | 0.580±.018 | 0.565±.013 | 0.595±.010 | 0.612±.021 | 0.621±.011 | 0.590±.017 |

**Figure 1**

| Conditions | | Start material | | Flotate | |
|---|---|---|---|---|---|
| Temp (ºC) | Press (psi) | Mass (g) | TOC (%) | Mass (g) | Yield (%) |
| 30 | 14.5 | 50.24 | 8.79 | 0 | 0 |
| 250 | 600 | 50.1 | 8.79 | 0.23 | 0.46 |
| 275 | 800 | 50.1 | 8.79 | 0.22 | 0.43 |
| 300 | 1250 | 50.3 | 8.79 | 0.05 | 0.11 |
| 325 | 2000 | 50.33 | 8.79 | 1.05 | 2.08 |

| Arranged data for chart | 25°C,14.5 psi | 250 C, 500 psi | 275 C, 800 psi | 300 C, 1250 psi |
|---|---|---|---|---|
| Flotate | 0 | 0.46 | 0.43 | 0.11 |
| Liquid-liquid extract | 0.5 | 0.04 | 0.16 | 0.02 |
| DCM:MeOH extract | 10.72 | 6.71 | 7.45 | 8.1 |

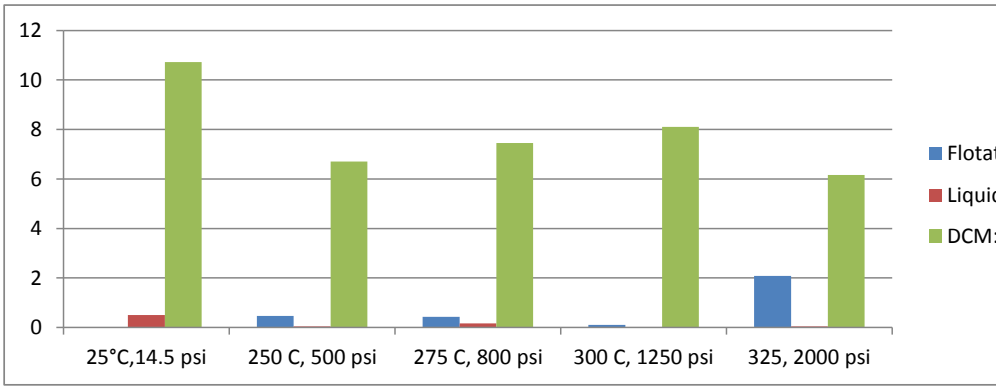


**Figure 2**

| Conditions | | Start material | | Flotate | |
|---|---|---|---|---|---|
| Temp (ºC) | Press (psi) | Mass (g) | TOC (%) | Mass (g) | Yield (%) |
| 30 | 14.5 | 50.24 | 8.79 | 0 | 0 |
| 250 | 600 | 50.1 | 8.79 | 0.23 | 0.46 |
| 275 | 800 | 50.1 | 8.79 | 0.22 | 0.43 |
| 300 | 1250 | 50.3 | 8.79 | 0.05 | 0.11 |
| 325 | 2000 | 50.33 | 8.79 | 1.05 | 2.08 |

| Arranged for chart | 25°C,14.5 psi | 250 C, 500 psi | 275 C, 800 psi | 300 C, 1250 psi |
|---|---|---|---|---|
| Flotate | 0 | 0.46 | 0.43 | 0.11 |
| Liquid-liquid extract | 0.5 | 0.04 | 0.16 | 0.02 |
| DCM:MeOH extract | 10.72 | 6.71 | 7.45 | 8.1 |

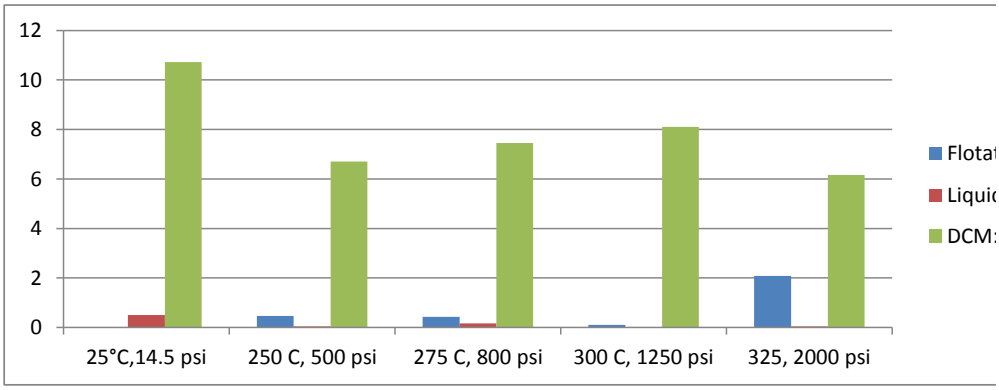


**Figure 3**
Click here to download high resolution image

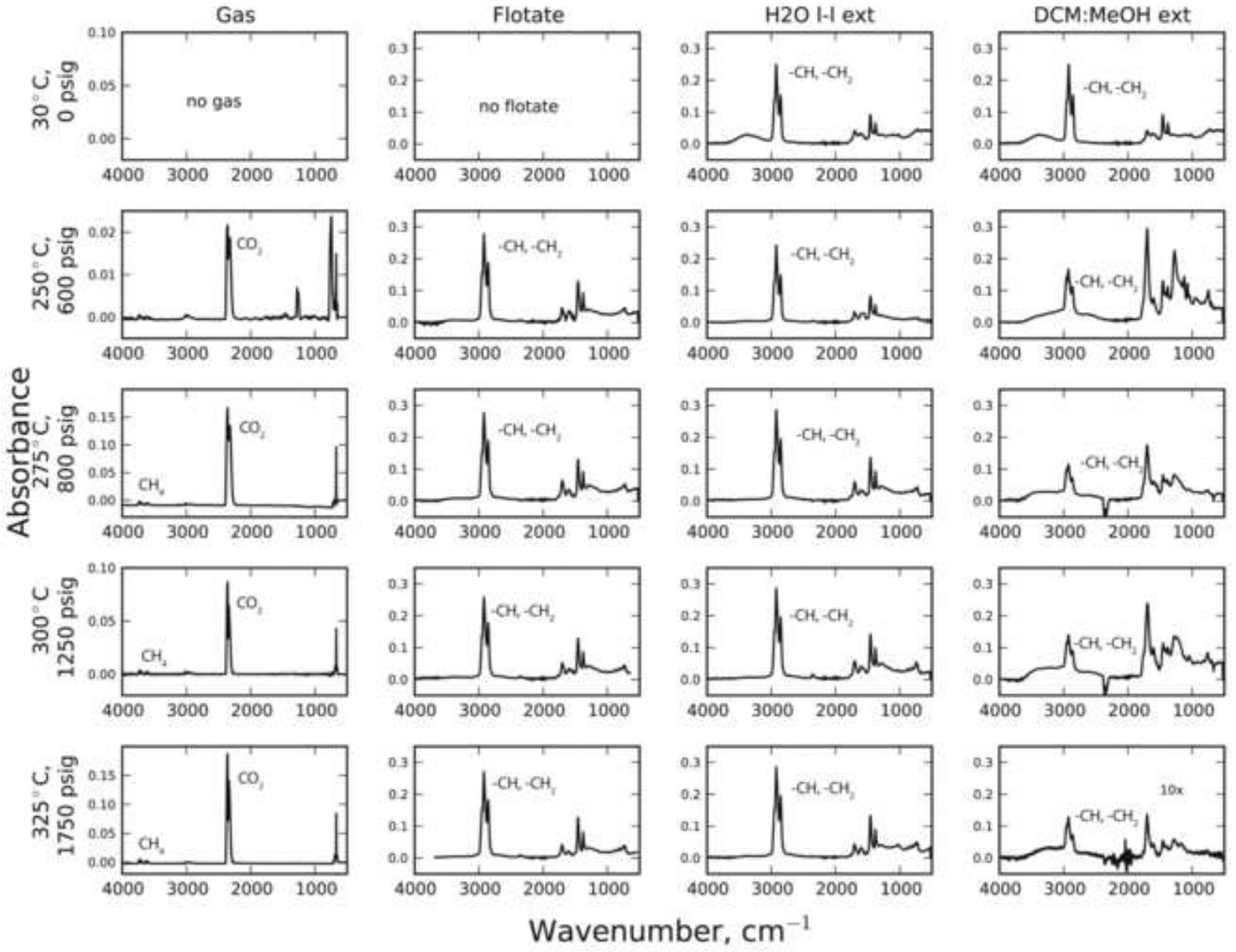


**Figure 4**
**Click here to download high resolution image**

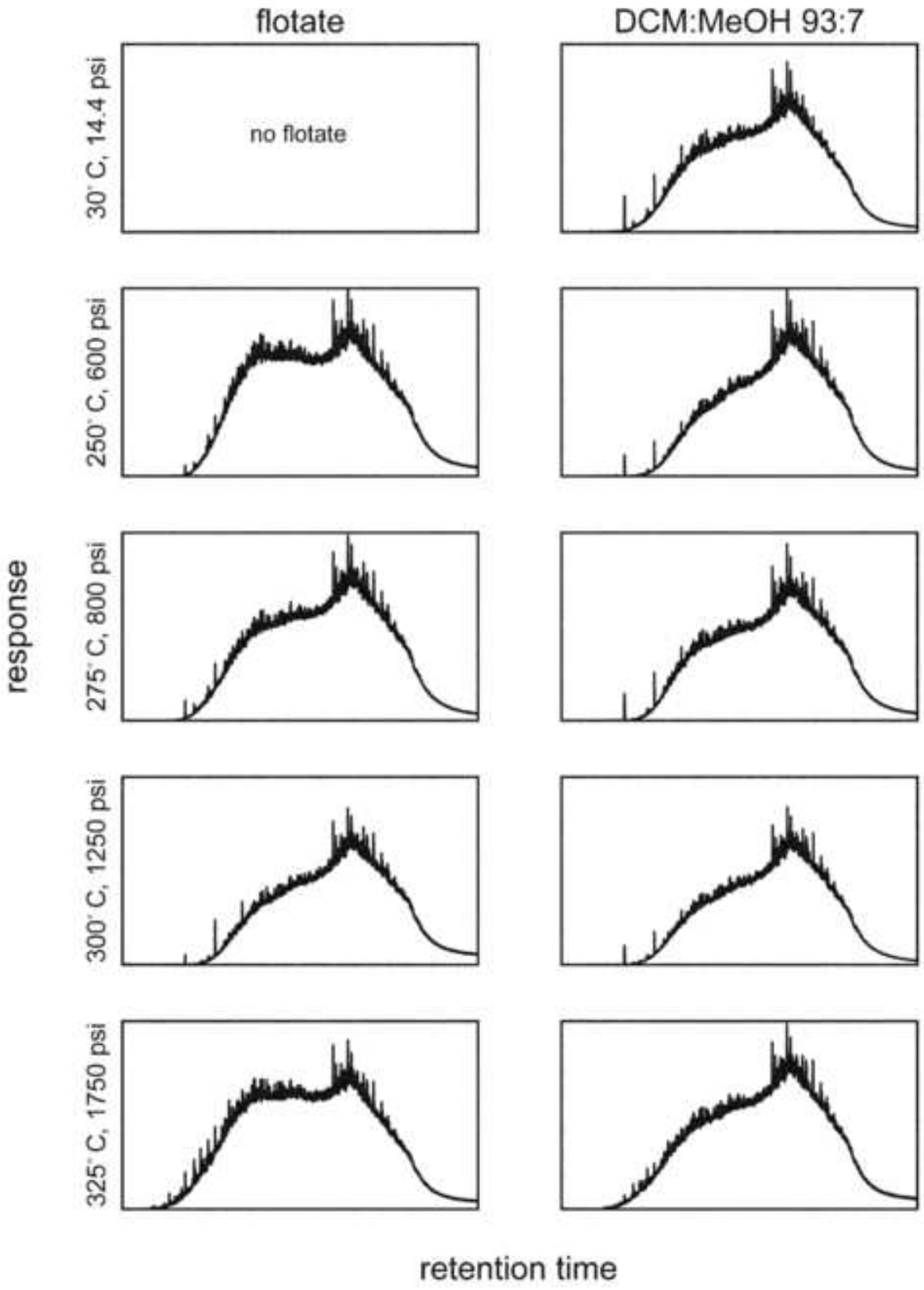


**Figure 5**
Click here to download high resolution image

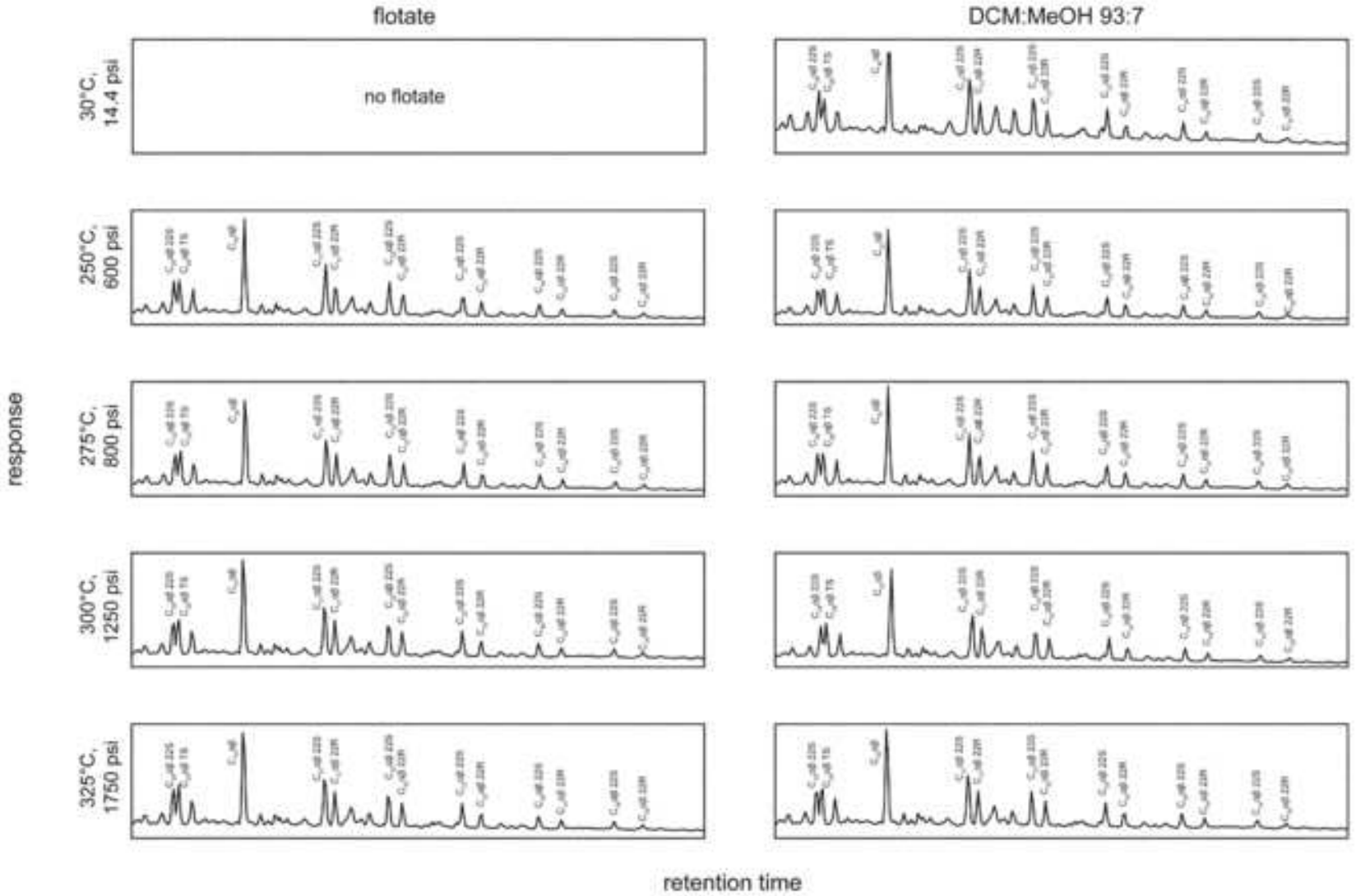


**Figure 6**
Click here to download high resolution image

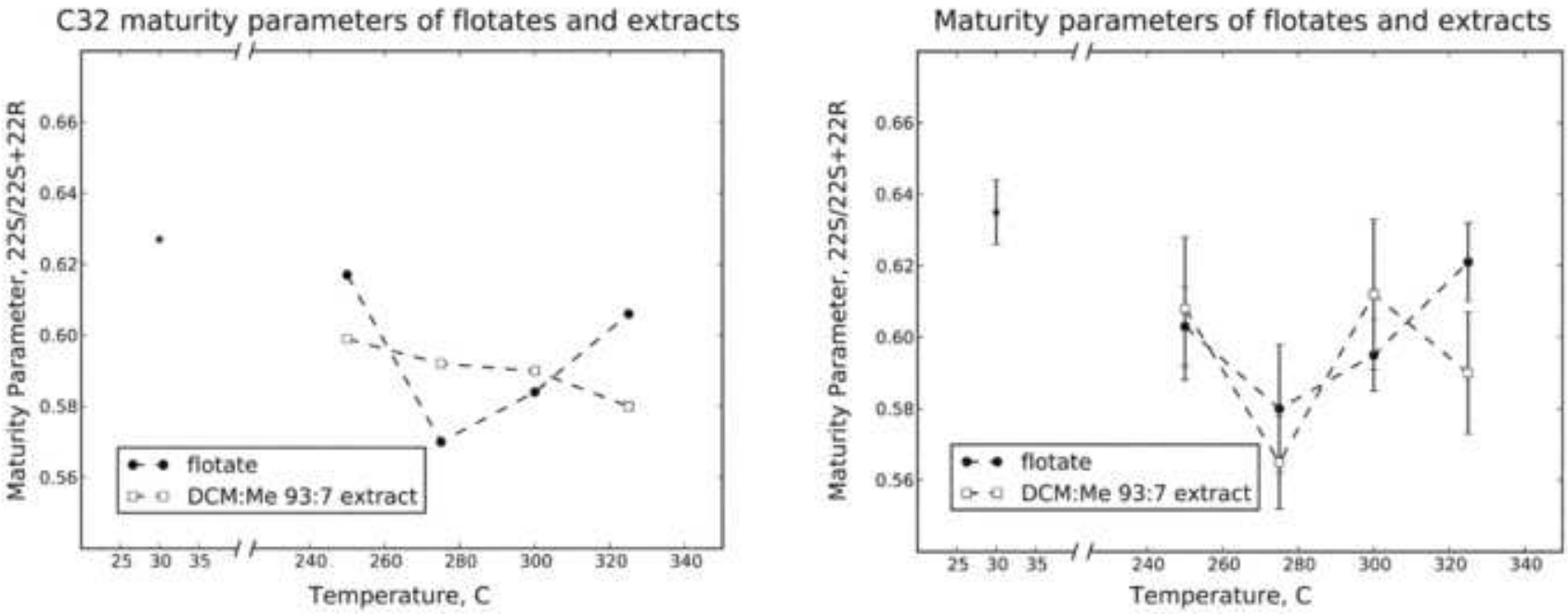


**Figure 7**
**Click here to download high resolution image**

